ACS ES&T Water

Open Access

pubs.acs.org/estwater

Article

Nontarget Analysis of Disinfection Byproducts Using Sequential Extraction and Elution

Anna Andersson,* Mourad Harir, Michael Gonsior, Norbert Hertkorn, Philippe Schmitt-Kopplin, Henrik Kylin, Ämma Pettersson, Felicia Larsson, and David Bastviken

Cite This: *ACS EST Water* 2026, 6, 2444−2457

Read Online

ACCESS | Metrics & More | Article Recommendations | Supporting Information

ABSTRACT: Disinfection byproducts (DBPs) formed upon drinking water treatment are often cytotoxic and genotoxic, and have been related to health risks, such as bladder cancer. Large DBPs, with more than two carbon atoms, are produced in large quantities and great diversity, and contribute substantially to observed toxicity, but their composition and structure remain largely unknown. While a few studies have explored high-resolution detection methods, we here focus on the extraction and elution procedures of these >2 carbon DBPs, before using negative electrospray ionization (ESI[−]) and detection by Fourier transform ion cyclotron resonance mass spectrometry (FT-ICR MS). Samples were collected from three drinking water treatment plants (DWTPs) in Sweden, of which two use hypochlorite and one uses monochloramine for disinfection. A reversed-phase SPE sorbent (Hyper Sep) showed high complementarity with a hybrid carbon sorbent (Carbon S), which captured a subset of polar saturated DBPs not retained by the commonly used reversed-phase materials. Stepwise elution using solvents of varying polarity reduced sample complexity and ionization suppression and further extended the DBP diversity detected. Extraction at pH 8, investigated for one DWTP, also extended DBP diversity but that impact was smaller. The classic methanol elution on reversed phase may miss proportionally more DBPs in chloraminated drinking water.

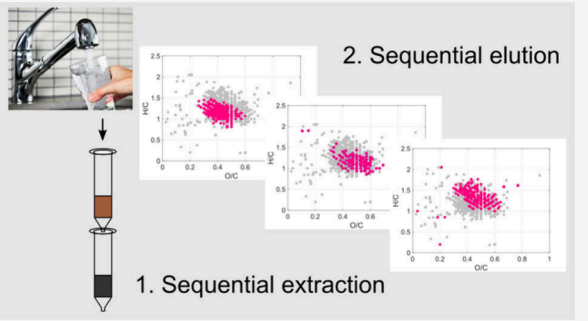

KEYWORDS: *drinking water, chlorination, chloramination, complex mixtures, extraction methods, FT-ICR MS*

1. INTRODUCTION

Disinfection byproducts (DBPs), an unintended consequence of chemical disinfection during drinking water production, were discovered in the 1970s.[1] Epidemiological studies have demonstrated various health risks associated with chlorine and chloramine treated drinking water, including bladder cancer[2] and adverse birth outcomes.[3,4] Well-known and often regulated DBPs include volatile trihalomethanes (THMs) and polar haloacetic acids (HAAs), containing one or two carbons, respectively. In general, most efforts have been placed on characterizing the low molecular weight (semi)volatile fraction of DBPs, constituting about 30% of total organic halogen (TOX) in chlorinated drinking water.[5] However, when developmental toxicity were measured on prepared DBP mixtures before and after purging, no significant difference was observed.[6] When toxic effects of DBPs have been compared between the purgeable (volatile) and nonpurgeable (non-volatile) fraction, i.e., adsorbable organic halogens (AOX) remaining after a set time of purging, the nonpurgeable fraction showed enhanced cytotoxicity, oxidative stress induction and genotoxicity, for both controlled lab-scale chlorination[7] and chlorinated and chloraminated tap water.[8] Recent studies of one or two carbon containing DBPs found no correlation between these DBPs and total cytotoxicity.[9] In fact, opposite trends were observed for cytotoxicity and the 1−2 carbon DBPs. In the nonpurgeable fraction only 4−16% of the halogenated compounds could be attributed to known DBPs.[8] Hence, there is a need to improve enrichment methods and chemical characterization of unknown nonvolatile >2 carbon DBPs.

Extractions are a vital preconcentration step in most analyses of organic compounds. Most extractions are highly selective leading to a bias in the later analysis even if done with highly advanced separation and/or detection methods.[10−13] Despite development of advanced methods including solid phase extraction (SPE) this issue remains due to the intrinsic molecular selectivity of different SPE materials. This is causing concern in DBP studies given the great DBP diversity spanning large ranges in molecular size, charge characteristics and hydrophobicity.[14] We therefore explore the use of multiple SPE columns optimized for the capture of different molecular characteristics in series.

Received: December 12, 2025
Revised: March 6, 2026
Accepted: March 6, 2026
Published: April 1, 2026

Mixed-mode sorbents combine materials to retain more diverse molecules based on multiple mechanisms, such as reversed-phase interactions, adsorptive capacity and anion or cation exchange interactions.[15] Because of the additional sorption mechanisms, a mixed-mode sorbent has the potential to extend the numbers and diversity of DBPs sorbed to an individual SPE. However, some polar DBPs will probably escape capture by reversed-phase sorbents, which is why sequential SPE extractions, adding a sorbent with different sorption capacity in sequence, could further enhance the sorption of nonvolatile DBPs. In natural organic matter (NOM) characterization, sequential extraction increased the number of detected features with 50%, compared to single SPE extraction.[16] A sequential extraction would specifically improve detection of the DBP pool not captured by Bond Elut PPL, the styrene-divinylbenzene copolymer which most DBP nontarget studies have used.[17−20]

The selection of sorbed DBPs eluted with organic solvents depends on the physicochemical properties of molecules and extraction solvents alike. DBPs are preferentially eluted when critical physicochemical parameters match, i.e., dipole moment, dielectric constant, or polarity.[15] Selective extraction will decrease mixture complexity, sort DBPs according to desired properties, and will affect ionization selectivity in eluates.[21] Hence, consolidated mass spectra from several solvent fractions will overall detect more numerous and chemically more diverse compounds than those observed in single fractions.

For example, Bond Elut PPL extraction of dissolved organic matter (DOM), using stepwise elution applying gradients of methanol/water ratios (20:80, 50:50, and 100:0), captured 50% more molecular formulas using electrospray ionization (ESI^-)-Fourier transform ion cyclotron resonance mass spectrometry (FT-ICR MS), compared with the conventional one-step elution,[22] i.e., with one solvent only. Because polarity of a compound and its ionization efficiency in negative ionization mode are related, i.e., polar molecules are more readily ionized, molecules in the less polar fraction can be better detected by ESI^--FT-ICR MS because they are no longer competing with the readily ionized components that were separated in the polar fraction.[22] Stepwise elution of Suwannee River natural organic matter sorbed to Bond Elut PPL with methanol/water (50:50) and methanol and methanol/dichloromethane (50:50), increased DOM recovery and allowed detection of a weakly polar fraction (~5.7% of total organic carbon (TOC)) that could not be detected with one-step elution.[23] Even when DOM sorbed to Bond Elut PPL is eluted with a single solvent, methanol, but collected separately in equal aliquots, the molecular complexity in each extract is reduced, which increase the disposable resolution for characterization.[21] Previous published works on DBP determination using SPE and FT-ICR MS all use one-step elution, typically with methanol.[24] Stepwise elution approaches, like those tested for DOM characterization, therefore have the potential to further increase the diversity of detected DBPs leading to more comprehensive exposure analyses.

FT-ICR MS offers high mass resolution and mass accuracy, and is a suitable tool to detect hundreds of molecular compositions of the nonvolatile DBP fraction.[25] This technique has revealed nonvolatile DBPs formed by different disinfectants and precursors and examined the consequences of various treatment processes on DBP formation[18,19,26−31] and will be used to determine DBPs in this study.

In this work, we connect two mixed-mode SPE sorbents, not used in previous DBP isolation and designed to extend the polarity range, in sequence, and use a stepwise elution procedure to extend the determination of nonvolatile, unknown DBPs formed in full-scale drinking water treatment applying chlorine or chloramine. We hypothesize that this will allow for more comprehensive detection of DBP composition and thereby also more comprehensive DBP exposure analyses.

2. METHODS

2.1. Methodology of Extraction and Elution

We selected Hyper Sep Retain CX and Bond Elut Carbon S/PSA for this study together with the commonly used Bond Elut PPL for comparison. Hyper Sep is a mixed phase, highly porous polystyrene divinylbenzene material modified with sulfonic acid functional groups and functions through both reversed-phase extraction and weak cation exchange. It has high recovery of a broad range of dissolved organic carbon (DOC) and nitrogen (DON) molecules.[32] This sorbent is highly interesting to improve detection of unknown, particularly nitrogen-containing DBPs (N-DBPs) that contribute substantially to the toxicity among known DBPs.[33,34] Except from the mixed phase, the particle size of Hyper Sep (30−50 μm) is smaller compared to the commonly used Bond Elut PPL (125 μm) and the average pore diameter is larger for Hyper Sep (83 Å) compared to Bond Elut PPL (0.9 Å).[32] A smaller particle size can increase extraction efficiency, and a larger pore diameter can improve accessibility to the stationary phase, especially for large molecules.[35] In a previous study comparing DOM extraction of Hyper Sep and Bond Elut PPL, the DOC recovery was similar between the cartridges, while Hyper Sep extracted a larger diversity of DOM assessed using FT-ICR MS.[32]

Bond Elut Carbon S/PSA is an advanced hybrid carbon material mixed with an alkylated amine sorbent (PSA) that contains two different amino functionalities. This was expected to improve the extraction of polar compounds. Carbon S also has a mixed phase functionality, through both adsorption to the carbon material and weak anion exchange. Carbon S was placed in sequence after Hyper Sep to capture polar DBPs not sorbing to Hyper Sep. A carbon based sorbent, such as graphitized carbon, seems not previously tested for DBP determination with FT-ICR MS.[17] In sequence to Bond Elut PPL, a Cellulose cartridge was tested for its potential to sorb polar DBPs based on hydrogen bond interactions.

To elute the sorbed DBPs, the following solvents were used for stepwise elution following a gradient of polarity: water/methanol (50:50), methanol, acetonitrile, and methanol/pentane (50:50). In addition, methanol with 1 mM KOH was used to elute cations sorbed to Hyper Sep[32] and methanol with 1% NH_4OH to elute anions sorbed to Carbon S. The purpose of the elution sequence was to improve desorption of DBPs from the SPE phase, i.e., improved desorption of polar DBPs (water/methanol, 50:50) and improved desorption of hydrophobic or large DBPs binding strongly to the reversed-phase (methanol/pentane, 50:50). Apart from an overall enhanced elution of sorbed DBPs, the stepwise elution was pursued to improve chemical characterization by FT-ICR MS (used as detection method; see below) through decreased ionization competition[36] among DBPs present in each fraction.

The pH impacts on the molecules' charged or uncharged state determines extraction behavior. Samples were lowered to pH 2.5 using 3 M hydrochloric acid (puriss PA), which leads to protonation of many carboxylic acids in DOM that are negatively charged at the original sample pH, enabling retention through hydrophobic interactions with the reversed-phase. We investigated pH-dependence of DBP sorption at pH 2.5 and 8 for one of the DWTPs (Borg; described below), because sequential extractions at different pH have also shown potential to extend the chemical diversity of detected DBPs.[37]

2.2. Description of the Three DWTPs

The three DWTPs included in the study are Råberga, Berggården, and Borg. Råberga and Berggården are located in Linköping but are using different source waters. Source water for Råberga is the humus-rich River Stångån with a forested catchment. The treatment of drinking water includes coagulation using Ekoflock 90, i.e., poly aluminum chloride, followed by rapid filtration through granular activated carbon

https://doi.org/10.1021/acsestwater.5c01469
ACS EST Water 2026, 6, 2444−2457

Table 1. Disinfectant Used and Bulk Characteristics of Water Sampled[a]

DWTP	disinfectant used	temp, C°	pH	tot. chlorine, mg L^{-1}	TOC, mg L^{-1}	UVA_{254}, cm^{-1}	UVA_{420}, cm^{-1}
Råberga	NaOCl	11.6	8.5	0.16	3.1	0.057	0.002
Berggården	NaOCl	7.0	8.3	0.11	2.2	0.039	0.002
Borg	NH_2Cl	1.2	8.0	0.25	4.8	0.061	0.002

[a]Temperature, pH, and total residual chlorine were measured in drinking water leaving the DWTPs; TOC, UVA_{254}, and UVA_{420} were measured in samples collected prior to chemical disinfection.

(GAC), slow sand filtration, UV disinfection, and disinfection with sodium hypochlorite. The source water at Berggården is River Motala Ström whose catchment is dominated by agriculture, and the water contained less allochthonous chromophoric DOM (CDOM). Here drinking water production requires less NOM removal and consists of rapid and slow sand filtration followed by UV disinfection and disinfection with sodium hypochlorite. The source water at Borg is also River Motala Ström, 50 km downstream of the intake for Berggården and after having passed two lakes surrounded by forest and agricultural areas. This water has higher levels of organic matter than at the intake for Bergården. The treatment at Borg includes coagulation using $Al_2(SO_4)_3$ followed by GAC filtration, slow sand filtration, UV disinfection and disinfection with chloramine. In both Råberga and Borg, GAC was operated as a biological filter to remove the undesired taste and odor. Bulk characteristics, including total organic carbon (TOC) and UVA_{254} of water samples collected at the three DWTPs, are presented in Table 1.

2.3. Sample Collection and Preparation

Water samples (1 L) were collected in October and November 2023 (Råberga and Berggården) and February 2024 (Borg). Two points during drinking water production were sampled: right before hypochlorite or chloramine addition and final drinking water, i.e., the drinking water leaving the DWTPs. Water samples were extracted immediately after collection by first adjusting pH to 2.5 using 3 M HCl (puriss PA). The potential impact of adduct formation from the added chloride was avoided through formic acid water washing of cartridges before elution.[38] At Borg, final water was also extracted at pH 8 to investigate DBPs isolated and detected at original pH. The SPE cartridges Hyper Sep (500 mg, 6 mL), Carbon S (500 mg, 6 mL), PPL (500 mg, 6 mL), and Cellulose (300 mg, 3 mL) were conditioned using methanol (6 mL, LiChrosolv) and acidified ultrapure water (6 mL, pH 2.5, LiChrosolv hypergrade). Hyper Sep was placed on top of Carbon S and PPL on top of Cellulose, on a visiprep manifold (12-port, Supelco). Water samples and cartridges were connected by Teflon tubing. Triplicate samples were extracted through Hyper Sep and Carbon S and one replicate sample through PPL and Cellulose for comparison. Exact volumes of water extracted were recorded (Table S1), and flow rates were kept below 5 mL/min to ensure enough time for interaction with the SPE sorbents. Blanks of 0.1% formic acid water (Ultra CHROMASOLV, Sigma A, 100 mL) were run through all SPE systems at all occasions.

After extraction, the cartridges were put individually on a larger visiprep manifold (24-port, Supelco), washed using 0.1% formic acid water (6 mL, Ultra CHROMASOLV, Sigma A) and dried with nitrogen gas, connected to a visidry system (24-port, Supelco), for ∼15 s. Elution (6 mL) was performed stepwise, using multiple solvents, collecting extracts (6 mL) from each solvent in separate vials (Figure 1). Figure 1 illustrates the Hyper Sep and Carbon S sequences; the same stepwise elution was applied for the PPL and Cellulose sequence. The order of elution was (1) water (LiChrosolv hypergrade): methanol (LiChrosolv for HPLC) 50:50 (v/v), (2) methanol (LiChrosolv for HPLC), (3) acetonitrile (LiChrosolv), (4) methanol (LiChrosolv for HPLC):*n*-pentane (LiChrosolv) 50:50 (v/v), (5) methanol (LiChrosolv for HPLC) containing 1 mM KOH to Hyper Sep cartridges and 6) methanol (LiChrosolv for HPLC) containing 1% ammonium hydroxide to Carbon S cartridges. For DWTP Råberga, sampled first, M-KOH was eluted prior to 50:50, v/v, methanol:*n*-pentane, as the methanol:*n*-pentane elution was not decided upon until the second sampling campaign. These fractions are hereafter named 50W50M, M, ACN, 50M50P, M-KOH, and M-NH_4OH in figures, tables, and text. Extracts were stored in freezer (−20 °C) until chemical analysis.

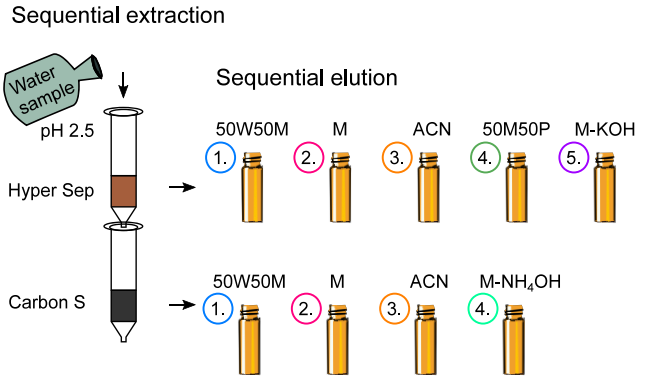

Figure 1. Schematic overview of the sequential extraction and elution. 50W50M, water:methanol (50:50, v/v); M, methanol; ACN, acetonitrile; 50M50P, methanol:pentane (50:50, v/v); M-KOH, methanol containing 1 mM KOH; and M-NH_4OH, methanol containing 1% NH_4OH.

2.4. FT-ICR MS Analysis

Characterization of DBPs in different fractions was done with a Bruker SolariX 12 T FT-ICR MS, operated with electrospray ionization (ESI) in negative mode. Extracts were diluted to an optimal dilution for the ICR cell based on the TOC (Table 1) and volume extracted (Table S1), using methanol. Extracts collected first, i.e., 50W50M and M, from Hyper Sep and PPL in top of the sequences, contained most ionizable ions and were diluted the most. Carbon S and cellulose extracts were less diluted. The extracts collected last in the stepwise elution, i.e., 50M50P and M-KOH, were run at near or at original concentration. Flow rate and spray current were set to 2 μL min^{-1} and −3.6 kV and 300 scans were acquired for each spectrum in a mass range of m/z 147.4 to 1000. Methanol blanks were run between extracts from the different DWTPs, i.e., every 15 extract, and method blanks were run before sample extracts. Mass spectra were internally calibrated against reference mass lists of NOM (Hyper Sep, PPL, Carbon S) and fatty acids (Cellulose) allowing mass errors <0.2 ppm.

2.5. Data Analysis

2.5.1. Filtration and DBP Verification. Mass lists from each spectrum were used to assign molecular formulas with software developed in-house at Helmholtz Munich, applying the following element criteria: $^{12}C_{0-100}$, $^{1}H_{0-\infty}$, $^{16}O_{0-80}$, $^{14}N_{0-3}$, $^{32}S_{0-2}$, $^{35}Cl_{0-5}$, $^{79}Br_{0-5}$, $^{127}I_{0-5}$.[26] The assigned formulas were filtered by applying the nitrogen rule and keeping formulas obeying the following constraints: error range < 0.2 ppm and > −0.2 ppm, intensity > 3,000,000, H/C ≤ 2.5, O/C ≤ 1.2, C > 0, O > 0, H (in neutral form) > 0, DBE ≥ 0 and experimental mass ≤ 800. The numbers of nitrogen and sulfur atoms were restricted to two and one, respectively. Furthermore, the second stable isotope of chlorine ^{37}Cl and bromine ^{81}Br was used to systematically verify halogenated formulas;[26] formulas containing ^{35}Cl and ^{79}Br were considered verified only if the corresponding mass peaks with ^{37}Cl or ^{81}Br was present in the original mass list (mass error <0.2 ppm). Further data analysis was performed on verified halogenated formulas only. We recognized all verified halogenated formulas present in all the three replicates and removed verified

https://doi.org/10.1021/acsestwater.5c01469
ACS EST Water 2026, 6, 2444−2457

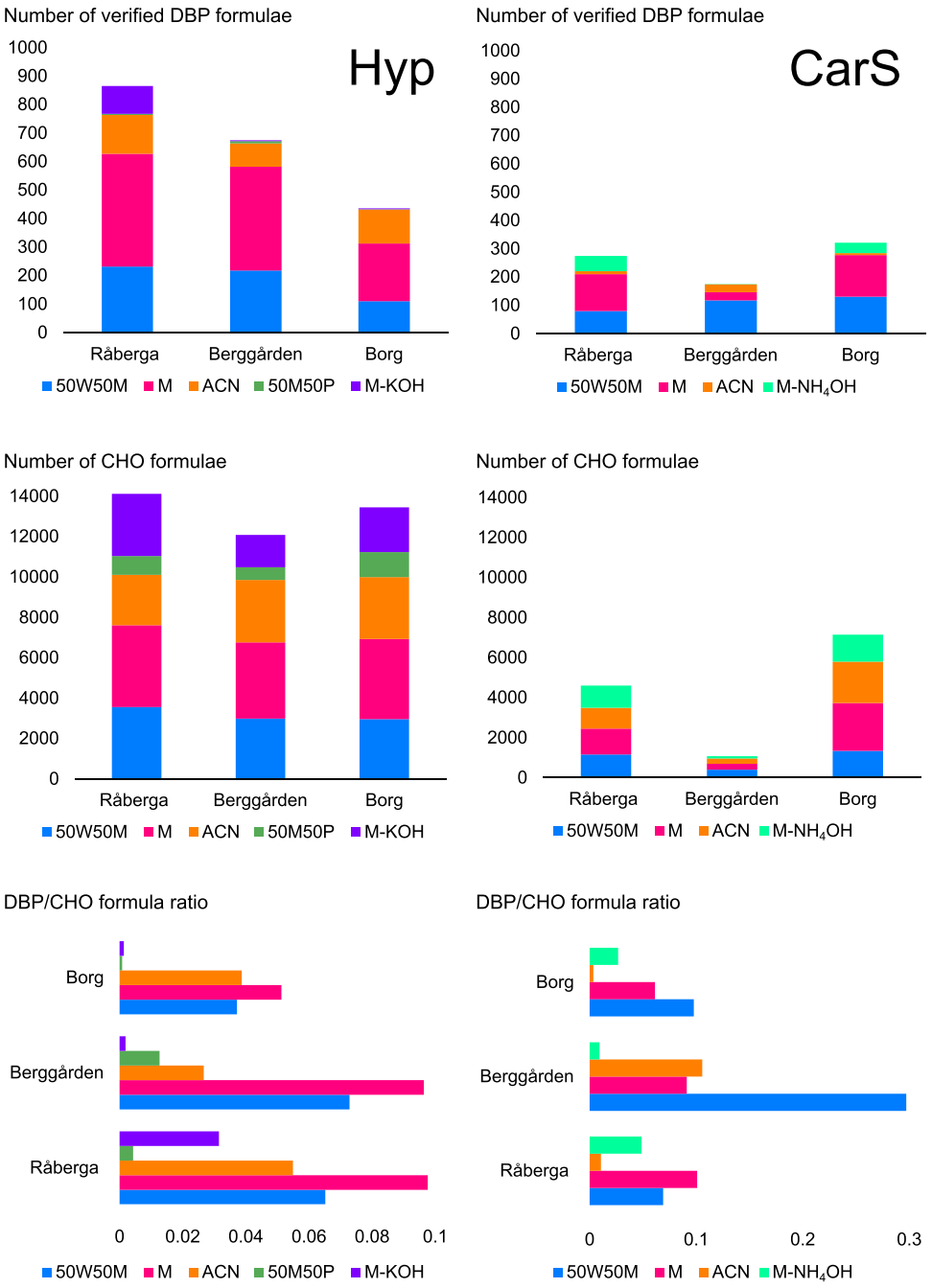

Figure 2. Overview of the number of verified DBP formulas and CHO formulas sorbed by Hyper Sep (Hyp) and Carbon S (CarS) detected in different fractions. Data represents three replicates added together. The third panel shows the DBP formulas to CHO formulas ratio for the different fractions.

halogenated formulas present in samples collected prior to chemical disinfection. Hence, the results focus on newly formed DBPs.

A parameter considering double bond equivalences (DBE), an indicator of the unsaturation of the carbon skeleton, subtracted by the number of oxygen atoms, [DBE−O], has been used to assess whether molecular formula assignments make sense from a chemical viewpoint.[39] Based on analysis among formulas with −10 > DBE−O > 10, a small number of DBP formulas (15) were removed from analysis based on unrealistically low numbers of hydrogen and oxygen atoms in relation to its carbon skeleton. Nitrogen-containing DBPs detected in ESI[−] at the settings used were few, i.e., the number of verified CHNOCl/Br/I formula were similar or less in final drinking water compared to before disinfection for all DWTPs and fractions. The analysis was therefore limited to DBPs containing carbon, hydrogen, oxygen, chlorine and/or bromine and iodine (CHOCl/Br/I). Note that only iodine DBPs that also included Cl and/or Br and could be verified by ^{37}Cl or ^{81}Br, were included; the unknown I-DBP pool might be larger. Data obtained in the ESI[+] mode might extend the detection of, e.g., N-DBPs but is outside the scope of this study. Verified DBPs in the Cellulose extracts detected by ESI[−] were few (<10) and not subject to further analysis. Hence, the focus of the further data analysis is on the extraction with Hyper Sep and Carbon S compared to the commonly used Bond Elut PPL.

2.5.2. Processing and Analysis. To compare the characteristics among DBPs detected in different fractions, DBP formulas were visualized using van Krevelen diagrams, H/C to mass, DBE/C to the number of oxygen, a modified aromaticity index (AI_{mod})[40] to the number of carbon and the average oxidation state of carbon (C_{OS}).[41] Double bond equivalences (DBE) can be described as the sum of unsaturated bonds and rings in a compound, and a high density of

https://doi.org/10.1021/acsestwater.5c01469
ACS EST Water 2026, 6, 2444−2457

Table 2. Average Weighted Compositions and Indices for Verified DBPs Extracted by Hyper Sep and Carbon S in Different Fractions at the Three DWTPs

	Hyper Sep					Carbon S			
elemental composition	50W50M	M	ACN	50M50P	M- KOH	50W50M	M	ACN	M- NH_4OH
Råberga									
mass weighted average [Da]	406.8	404.4	382.9	250.2	392.1	487.1	461.6	404.2	440.0
average DBE	7.4	7.6	7.5	5.0	7.6	6.6	7.4	5.9	7.1
average AI_{mod}	0.32	0.33	0.34	0.68	0.32	0.17	0.21	0.38	0.26
average carbon oxidation state (C_{OS})	−0.090	−0.34	−0.31	−0.13	−0.23	−0.50	−0.50	−0.35	−0.13
average DBE/C	0.44	0.42	0.43	0.62	0.44	0.31	0.35	0.37	0.39
average H [%]	42.4	45.1	44.7	36.8	43.9	48.7	48.2	46.2	44.6
average C [%]	36.7	37.6	37.8	44.3	37.3	35.0	35.8	37.5	36.1
average O [%]	17.7	14.6	14.9	10.9	16.2	13.9	14.1	10.5	16.5
average Cl [%]	2.9	2.4	2.6	0	2.4	2.3	1.9	4.7	2.6
average Br [%]	0.2	0.3	0.1	7.9	0.06	0.1	0	1.1	0.3
computed average H/C ratio	1.15	1.20	1.18	0.83	1.18	1.39	1.34	1.23	1.24
computed average O/C ratio	0.48	0.39	0.39	0.25	0.43	0.40	0.39	0.28	0.46
computed average Cl/C ratio	0.080	0.064	0.069	0	0.065	0.066	0.054	0.13	0.071
computed average Br/C ratio	0.006	0.008	0.002	0.18	0.002	0.003	0	0.030	0.008
Berggården									
mass weighted average [Da]	399.1	409.7	384.1	443.5	491.8	504.9	444.1	367.1	520.0
average DBE	6.8	7.5	7.1	4.1	7.1	5.3	5.8	0.9	20.0
average AI_{mod}	0.25	0.33	0.30	0.16	0.16	0.02	0.14	0.04	0.75
average carbon oxidation state (C_{OS})	−0.21	−0.30	−0.37	−0.84	−1.13	−0.49	−0.96	−1.23	−0.34
average DBE/C	0.40	0.42	0.40	0.21	0.28	0.26	0.27	0.06	0.69
average H [%]	44.8	44.7	45.9	52.7	53.4	49.0	53.1	59.3	32.0
average C [%]	35.7	37.6	37.0	33.8	36.7	33.6	35.7	31.0	58.0
average O [%]	17.1	14.8	14.6	9.5	7.4	13.9	9.1	6.9	2.0
average Cl [%]	2.4	2.5	2.5	3.6	2.6	3.3	1.9	2.3	8.0
average Br [%]	0.03	0.43	0.01	0.47	0	0.24	0.18	0.47	0
computed average H/C ratio	1.26	1.19	1.24	1.56	1.46	1.46	1.49	1.91	0.55
computed average O/C ratio	0.48	0.39	0.39	0.28	0.20	0.41	0.26	0.22	0.034
computed average Cl/C ratio	0.068	0.066	0.066	0.11	0.070	0.098	0.054	0.075	0.14
computed average Br/C ratio	0.001	0.012	0.0003	0.014	0	0.007	0.005	0.015	0
Borg									
mass weighted average [Da]	406.4	404.8	372.6	ND	558.8	432.2	439.5	467.8	381.7
average DBE	6.8	7.8	7.3	ND	11.6	7.0	6.8	11.9	8.6
average AI_{mod}	0.27	0.33	0.34	ND	0.31	0.21	0.19	0.52	0.47
average carbon oxidation state (C_{OS})	−0.29	−0.30	−0.30	ND	−0.84	−0.41	−0.38	−0.42	0.07
average DBE/C	0.39	0.43	0.43	ND	0.40	0.36	0.35	0.51	0.52
average H [%]	45.6	44.7	44.8	ND	48.2	47.2	47.3	43.2	40.5
average C [%]	36.0	37.6	37.7	ND	40.4	35.8	34.9	43.8	39.9
average O [%]	15.9	15.2	14.9	ND	8.2	15.0	15.8	9.4	16.7
average Cl [%]	2.4	2.3	2.6	ND	3.2	2.0	1.9	3.1	2.2
average Br [%]	0.2	0.2	0.04	ND	0	0.05	0.005	0.5	0.7
computed average H/C ratio	1.27	1.19	1.19	ND	1.19	1.32	1.35	0.99	1.01
computed average O/C ratio	0.44	0.40	0.40	ND	0.20	0.42	0.45	0.21	0.42
computed average Cl/C ratio	0.066	0.062	0.068	ND	0.079	0.057	0.055	0.070	0.055
computed average Br/C ratio	0.006	0.005	0.001	ND	0	0.001	0.0001	0.010	0.017

double bonds, i.e., a high DBE/C, can provide insight into the extent of aromatic structures. AI_{mod} is a more conservative approach to estimate aromatic characteristics, assuming that 50% of the molecular oxygen is bound with double-bonds and not contributing to aromaticity.[40]

Even when oxidation applies to specific carbon atoms, the average oxidation state (C_{OS}) of the entire molecules increases.[41] The C_{OS} was computed according to equation 1 where nH is the number of hydrogen atoms in neutral form and nO, nCl, nBr, nI and nC are the number of oxygen, chlorine, bromine, iodine, and carbon atoms, respectively.

$$C_{OS} = -[(nH \times 1) + (nO \times (-2)) + (nCl \times (-1)) + (nBr \times (-1)) + (nI \times (-1))]/nC \quad (1)$$

Two distinct plots depicted results focusing on presence or absence of DBP formulas in the different fractions: (1) studying each DBP fraction as a whole to investigate compositional shifts against the total DBP pool detected and (2) studying the composition of DBPs detected in each fraction, e.g., DBPs containing Cl_1, Cl_2, Cl_3, Br_1, Br_2, and so forth.

To investigate the overlap of DBPs detected in different fractions, elemental formulas were compared and visualized for each DWTP and cartridge using upset plots. These plots were used to simultaneously show (1) how many DBPs that were detected in each fraction and (2) which fractions hold high counts of unique DBPs, i.e., DBPs not detected in other fractions. Weighted averages of elemental compositions and the above-mentioned indices, based on all DBP

https://doi.org/10.1021/acsestwater.5c01469
ACS EST Water 2026, 6, 2444−2457

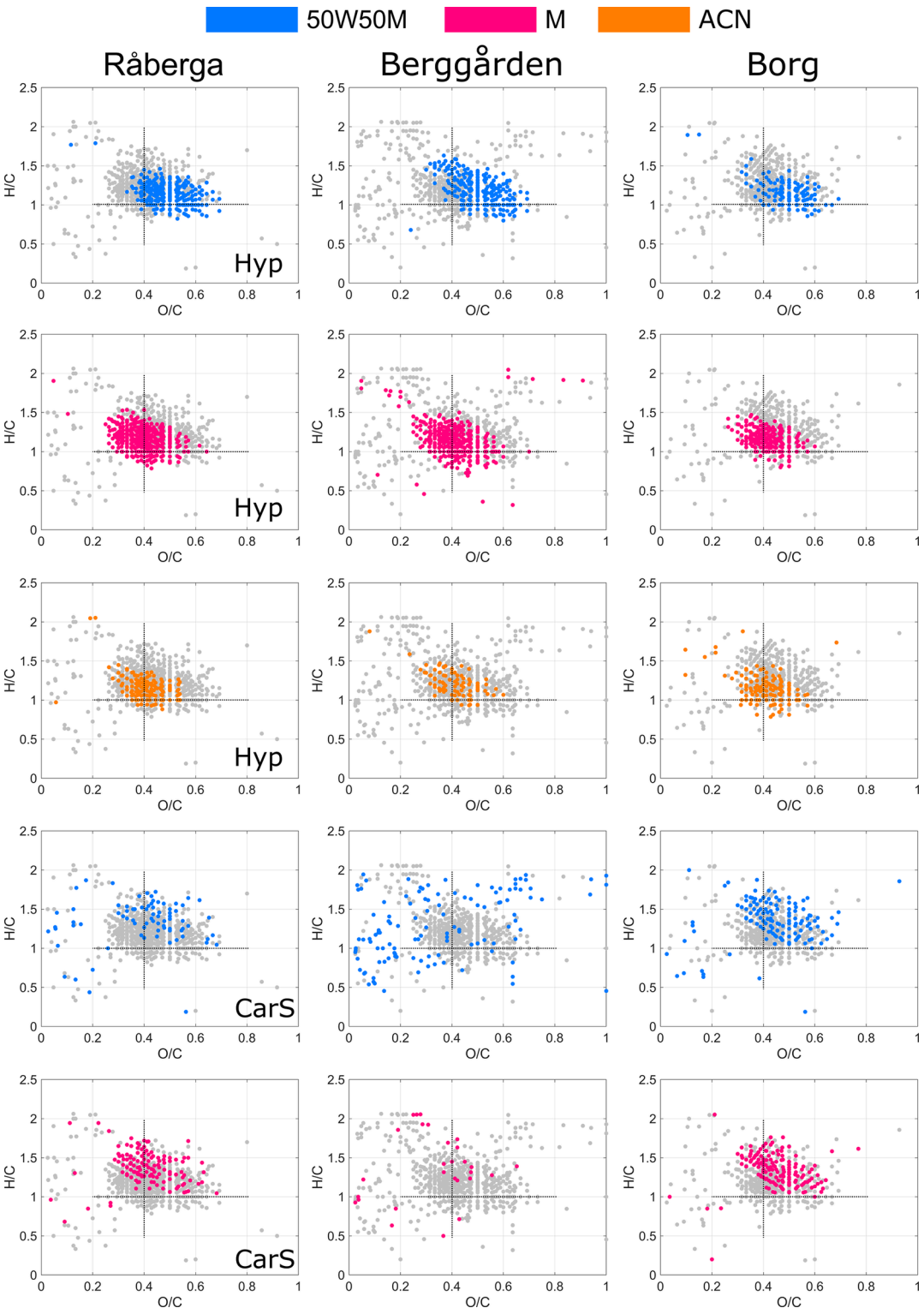

Figure 3. Van Krevelen diagrams of verified DBP formulas detected at the three DWTPs in different fractions, i.e., water:methanol (50:50, v/v) (50W50M), methanol (M), and acetonitrile (ACN), eluted on Hyper Sep (Hyp) and subsequent Carbon S (CarS) cartridges. The gray dots demonstrate all DBPs detected, with the DBPs detected in a fraction highlighted in different colors. The lines forming a cross are just reference points to facilitate detection of shifts.

compositions in a fraction, were calculated by computing individual mass peak amplitudes divided by the combined intensities of all mass peaks in the spectrum. All data processing were conducted using Matlab 2024.

3. RESULTS AND DISCUSSION

3.1. DBP Characterization of Different Fractions

DBP molecular formulas were verified in both Hyper Sep and Carbon S extracts, and a higher number of DBP formulas were sorbed to and eluted from Hyper Sep (Figure 2). Most DBPs

https://doi.org/10.1021/acsestwater.5c01469
ACS EST Water 2026, 6, 2444−2457

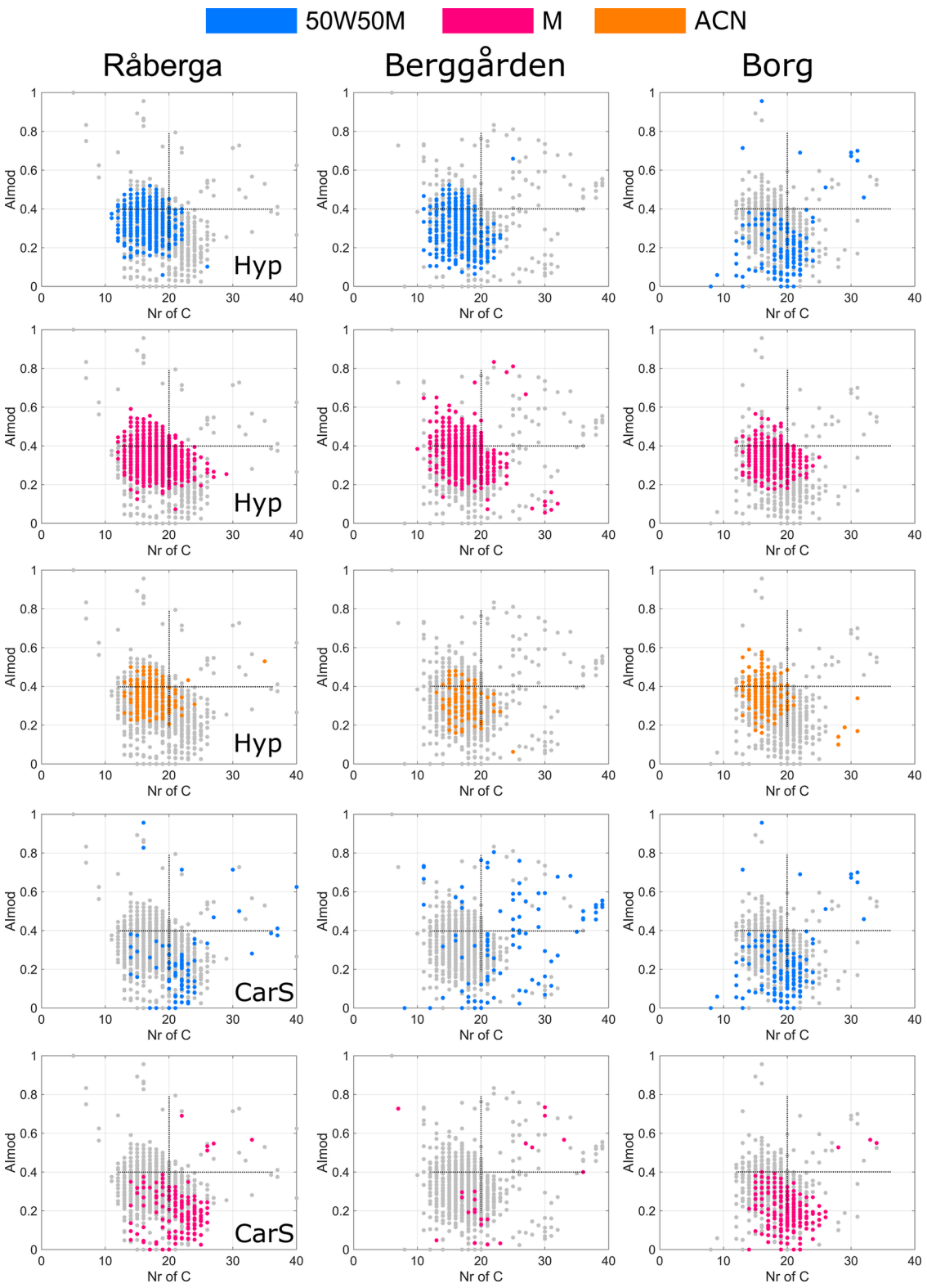

Figure 4. AI_{mod} against number of carbon plots of verified DBP formulas detected at the three DWTPs in different fractions, i.e., water:methanol (50:50, v/v) (50W50M), methanol (M), and acetonitrile (ACN), eluted on Hyper Sep (Hyp) and subsequent Carbon S (CarS) cartridges. The gray dots demonstrate all DBPs detected, with the DBPs detected in a fraction highlighted in different colors.

(72−86%) were detected in 50W50M and M fractions, indicating a predominance of moderately to highly polar species (Figure S1). At Borg DWTP, which uses chloramine for disinfection, a larger share of DBPs sorbed to Hyper Sep was detected in the ACN fraction, suggesting slightly different DBP formation under these disinfection conditions. Compared to DWTPs using hypochlorite, the DWTP applying chloramine yielded fewer DBPs in the Hyper Sep extracts, with similar numbers of CHO formulas, but more DBPs in the subsequent Carbon S extracts. This pattern suggests that chloramine

https://doi.org/10.1021/acsestwater.5c01469
ACS EST Water 2026, 6, 2444−2457

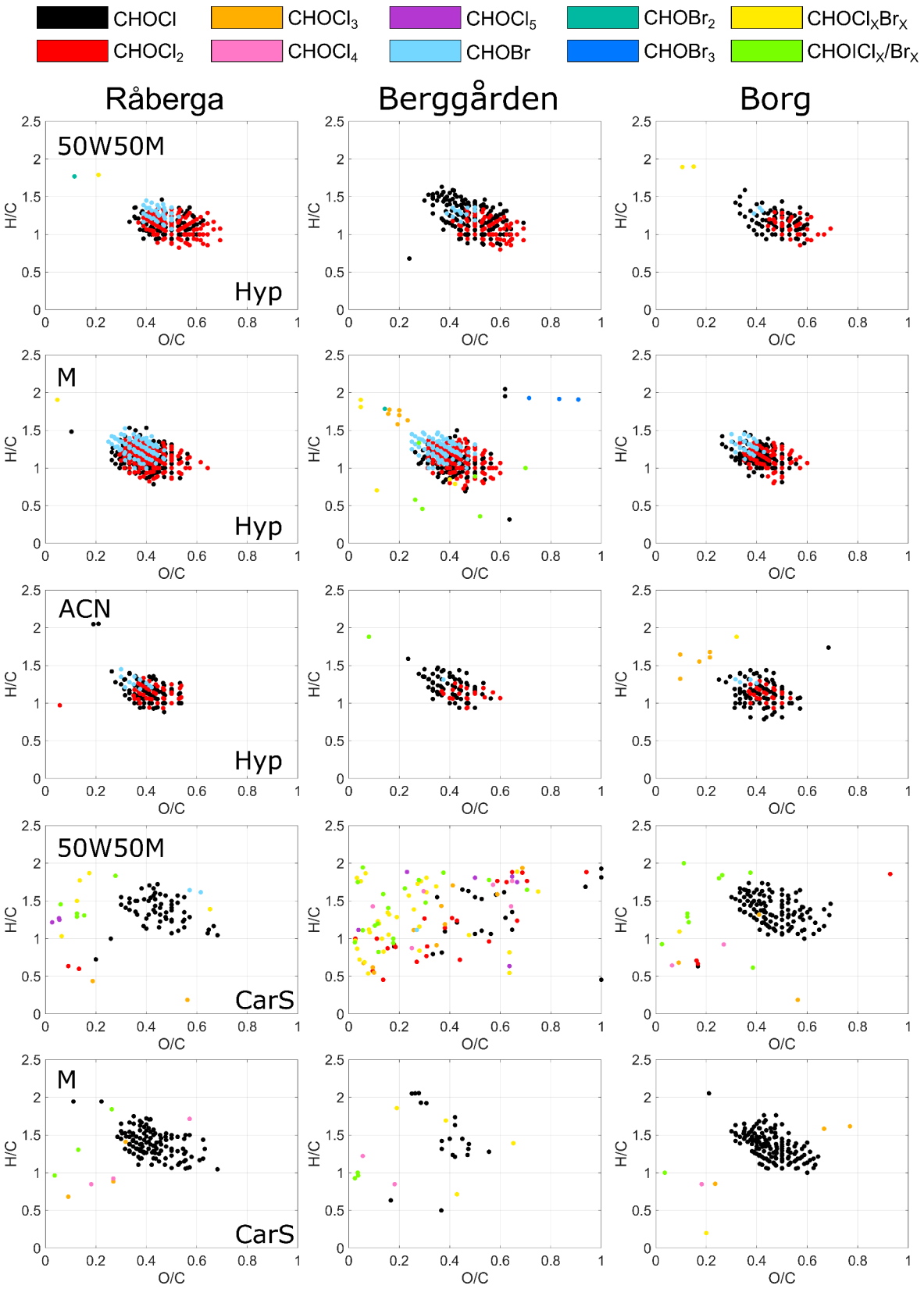

Figure 5. Characteristics of verified DBP formulas detected at the three DWTPs in different fractions, i.e., water:methanol (50:50, v/v) (50W50M), methanol (M), and acetonitrile (ACN), eluted on Hyper Sep (Hyp) and subsequent Carbon S (CarS) cartridges, displayed in van Krevelen diagrams.

disinfection favors the formation of DBPs not retained by the reversed-phase with greater affinity for Carbon S and detectable in ESI[−]. When comparing the numbers of DBP formulas and CHO formulas, the M fraction had the highest counts of DBP formulas in relation to CHO formulas in Hyper Sep extracts, while 50W50M had the highest counts in most Carbon S

https://doi.org/10.1021/acsestwater.5c01469
ACS EST Water 2026, 6, 2444−2457

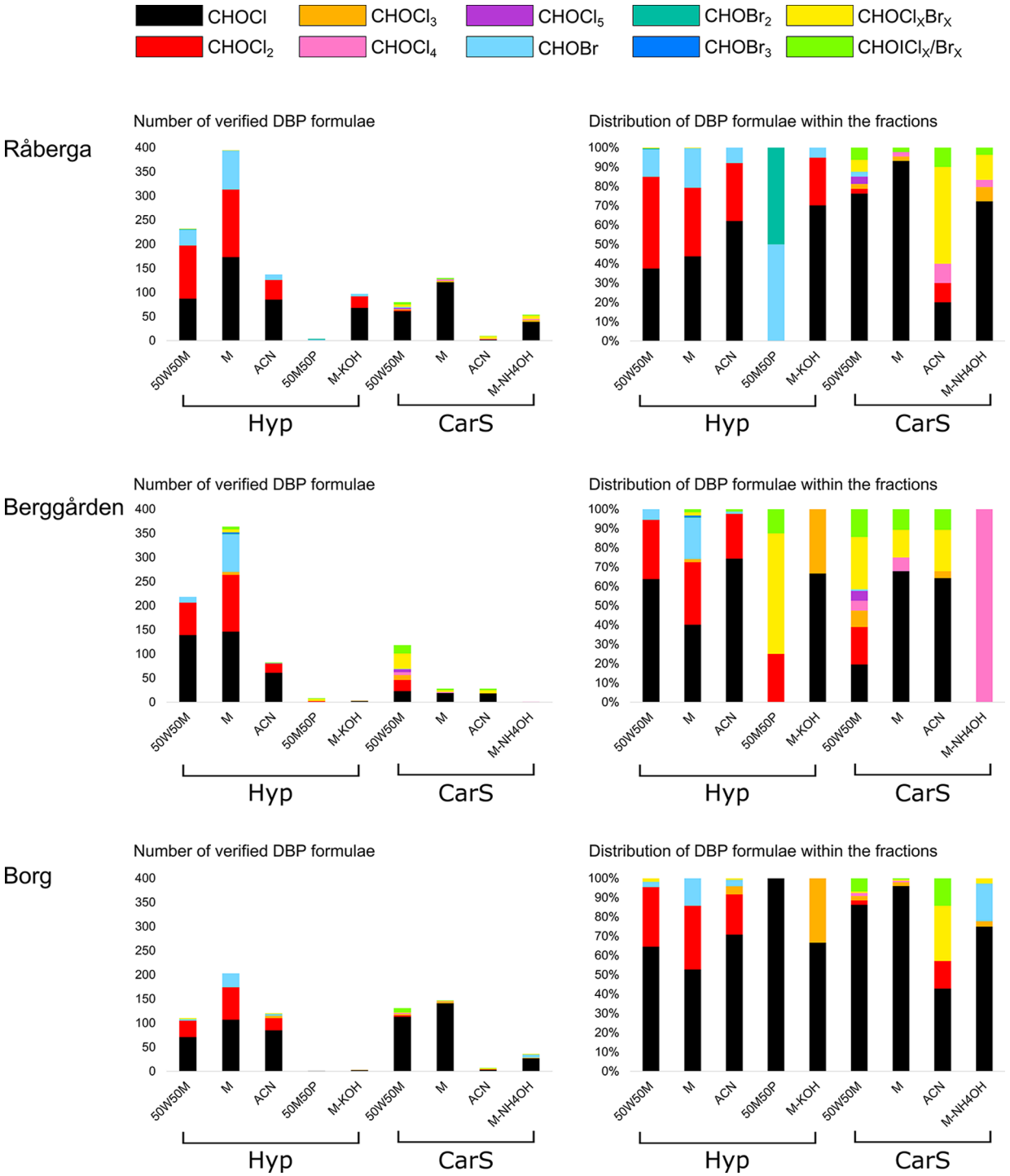

Figure 6. Characteristics of verified DBP formulas detected at the three DWTPs in different fractions, i.e., water:methanol (50:50, v/v) (50W50M), methanol (M), acetonitrile (ACN), methanol:pentane (50:50, v/v) (50M50P), methanol with 1 mM KOH (M-KOH) and methanol with 1% NH_4OH, eluted on Hyper Sep (Hyp) and subsequent Carbon S (CarS) cartridges.

extracts (Figure 2). Furthermore, the DWTP using chloramine had overall lower counts of detected DBPs in relation to CHO formulas, indicating that fewer DBPs were formed relative to the CHO diversity or that DBPs formed were not detected by the methods used. While considerable amounts of CHO formulas were detected in M-KOH extracts, DBP formulas were primarily detected in one plant. Least CHO and DBP formulas were detected in 50M50P extracts. Overall, the results indicate a strong influence of the disinfectant type on DBP polarity, sorption behavior, and overall molecular diversity. The weighted average elemental compositions and molecular indices of DBPs identified in the different fractions are summarized in Table 2.

3.1.1. The Hyper Sep Cartridge. For DBPs captured by the reversed-phase Hyper Sep cartridge, a clear shift was observed from higher O/C ratios among DBPs detected in 50W50M extracts toward lower O/C ratios among those detected in the M fractions (Figure 3, Table 2), reflecting the different polarity of these eluents. This shift was consistent across all DWTPs but

https://doi.org/10.1021/acsestwater.5c01469
ACS EST Water 2026, 6, 2444−2457

was most pronounced in those using hypochlorite. DBP formulas detected in the 50W50M fractions also exhibited a higher number of oxygen atoms (Figure S2) and higher average oxygen content (Table 2), compared to those detected in the M fraction. This is consistent with their enhanced polarity and stronger interactions with the stationary phase, leading to elution with the more polar solvent mixture. Additionally, a shift in relative (un)saturation was observed between these fractions, where DBPs in the M fractions had higher AI_{mod} compared to DBPs detected in the 50W50M fraction (Figure 4, Table 2), which agreed with the observation that methanol was required to elute some of the less polar but more unsaturated DBPs sorbed onto the Hyper Sep cartridge.

The degree of oxygenation did not change in the less polar ACN fraction, where DBPs showed lower mass (<450 Da) and overall, less diversity compared to 50W50M and M fractions (Figures 3 and 5 and Figure S3). Only a few DBPs were detected in the last and least polar fraction containing 50% pentane (50M50P) (Figures S4−S6). DBPs eluted with M-KOH were primarily detected in Råberga, indicating that the order of the elution may influence recovery. Nevertheless, DBPs detected in the M-KOH eluates were not chemically distinct from those in other fractions (Figures S4−S6).

3.1.2. The Subsequent Carbon S Cartridge. DBPs captured by Carbon S (receiving the output from the Hyper Sep cartridge) were primarily detected in the 50W50M, M, and M-NH_4OH fractions (Figure 3 and Figure S4). Apart from Berggården, no clear shift in polarity or saturation was observed between DBPs detected in 50W50M and M fractions from Carbon S. In contrast, chemically distinct DBPs were observed in the M-NH_4OH fraction, corresponding to DBPs eluted from the anion exchange function. Compared to DBPs extracted by Hyper Sep, those extracted by Carbon S generally showed higher mass (Figure S3, Table 2) and were more saturated, as indicated by higher H/C ratios and lower calculated aromaticity (Figures 3 and 4, Table 2). Specifically, DBPs sorbed to Carbon S were characterized by low DBE/C ratios and higher oxygen content (Figure S2), indicating that these DBPs were less hydrophobic and more polar than those sorbed to Hyper Sep. This likely explains why such DBPs passed through the Hyper Sep sorbent and highlights the presence of a pool of DBPs not captured by reversed-phase extraction alone. DBPs detected in Carbon S extracts were more similar between Råberga and Borg, despite the fact that the raw water at Berggården and Borg originates from a joint water source. These differences are likely explained by differences in NOM abundance and composition, which are also reflected in similar treatment stages at Råberga and Borg. In Berggården, a larger diversity of Carbon S DBPs was detected, especially in the 50W50M fraction. These DBPs were likely formed by different precursors present in this source water, e.g., saturated compounds assessed as protein-like fluorescence,[42] that did not absorb at 254 nm (Table 1). It is possible that these precursors were present also in Borg but that other precursors, i.e., UV absorbing molecules, that are more reactive toward the chemical disinfectant, were favored in DBP formation there.

The composition of DBPs is highly linked to their toxicological potential. For instance, halogen substitution strongly influences toxicity: brominated and iodinated DBPs are orders of magnitude more toxic than their chlorine-DBP analogue,[43] with iodine-containing DBPs often showing highest toxicity. Bromine-containing DBPs, mostly containing a single bromine atom, were predominantly sorbed by Hyper Sep and detected in the M fraction, while very few DBPs containing combinations of chlorine, bromine, or iodine were detected in Hyper Sep extracts (Figures 5 and 6, and Figures S7−S9). Instead, iodine-containing DBPs and mixed Cl−Br DBPs were captured by Carbon S and primarily detected in the 50W50M fraction.

3.2. DBP Overlap between Fractions and DWTPs

Among the DBPs sorbed by the Hyper Sep cartridge, the majority were detected exclusively in one fraction from a specific DWTP, *viz.*, 59, 75 and 64% in Råberga, Berggården and Borg, respectively. For all DWTPs, most DBPs were detected in the M fraction only, followed by DBPs found in the 50W50M fraction only (Figure 7). Among DBPs detected in multiple fractions, most were detected in the 50W50M and M fractions, demonstrating an overlap of DBPs detected in these fractions, especially for the DWTPs using hypochlorite. Each formula could potentially represent ∼260 different structural isomers[44] and the formula overlap might be explained by different isomers having different desorption behavior. Alternatively, the desorption of the overlapping formulas was incomplete by one solvent and continued with another. DBPs detected in the ACN fractions were often also detected in the M, 50W50M, and M-KOH fractions, i.e., for 94, 87, and 69% of the DBP formulas in Råberga, Berggården and Borg. However, at Borg, the plant using monochloramine, a considerable number of DBPs were detected only in the ACN fraction (Figure 7).

The 50M50P eluate contained few DBP formulas, with all but one unique to this fraction. In Råberga, four low-saturation DBPs (H/C: 0.5−1) containing one or two bromine atoms (e.g., $C_7H_5O_2Br_1$, $C_7H_4O_2Br_2$, $C_9H_9O_2Br_1$, and $C_9H_8O_2Br_2$) were detected only in this fraction (Figure S8). Differences in spectral amplitude between cold and room-temperature injections likely reflect pentane's high volatility, affecting signal intensity but not the elution of low-polarity DBPs. These results highlight that low-polarity solvents, whether neat or in mixtures with more polar solvents, are important for stepwise elution methods. Decreased impact of pentane on ionization after methanol dilution might improve the detection limit. Also, ESI[−] might not be optimal for some of the less polar DBPs eluted with 50M50P and that other methods, such as APPI or APCI might be required to detect them. In contrast, few unique DBPs were detected using M-KOH to elute compounds bound to the cation exchange, indicating that this elution stage did not increase the chemical diversity.

For DBPs sorbed by the Carbon S cartridge, 85, 98 and 76% were unique to a single fraction in Råberga, Berggården and Borg, respectively; sequential elution led to even more distinct fractions for this sorbent than Hyper Sep (Figure 7). In Råberga and Borg, most DBPs were detected solely in the M fraction, while in Berggården, most DBPs were detected in the 50W50M fraction only, potentially linked to the different NOM characteristics of the source water in Berggården. In addition, at Berggården, few DBPs were detected in the M-NH_4OH fraction in comparison to the other DWTPs.

The low overlap of DBPs detected by Hyper Sep and Carbon S, (9, 2 and 15%) for Råberga, Berggården, and Borg, respectively, shows the complementarity of the two sorbents and the broader diversity of compounds captured when they are combined. A comparison of the overlap between the three DWTPs revealed that a higher proportion of unique DBPs, i.e., compounds detected in only one single DWTP, was found in the Carbon S extracts (74%) than in the Hyper Sep extracts (40%).

https://doi.org/10.1021/acsestwater.5c01469
ACS EST Water 2026, 6, 2444−2457

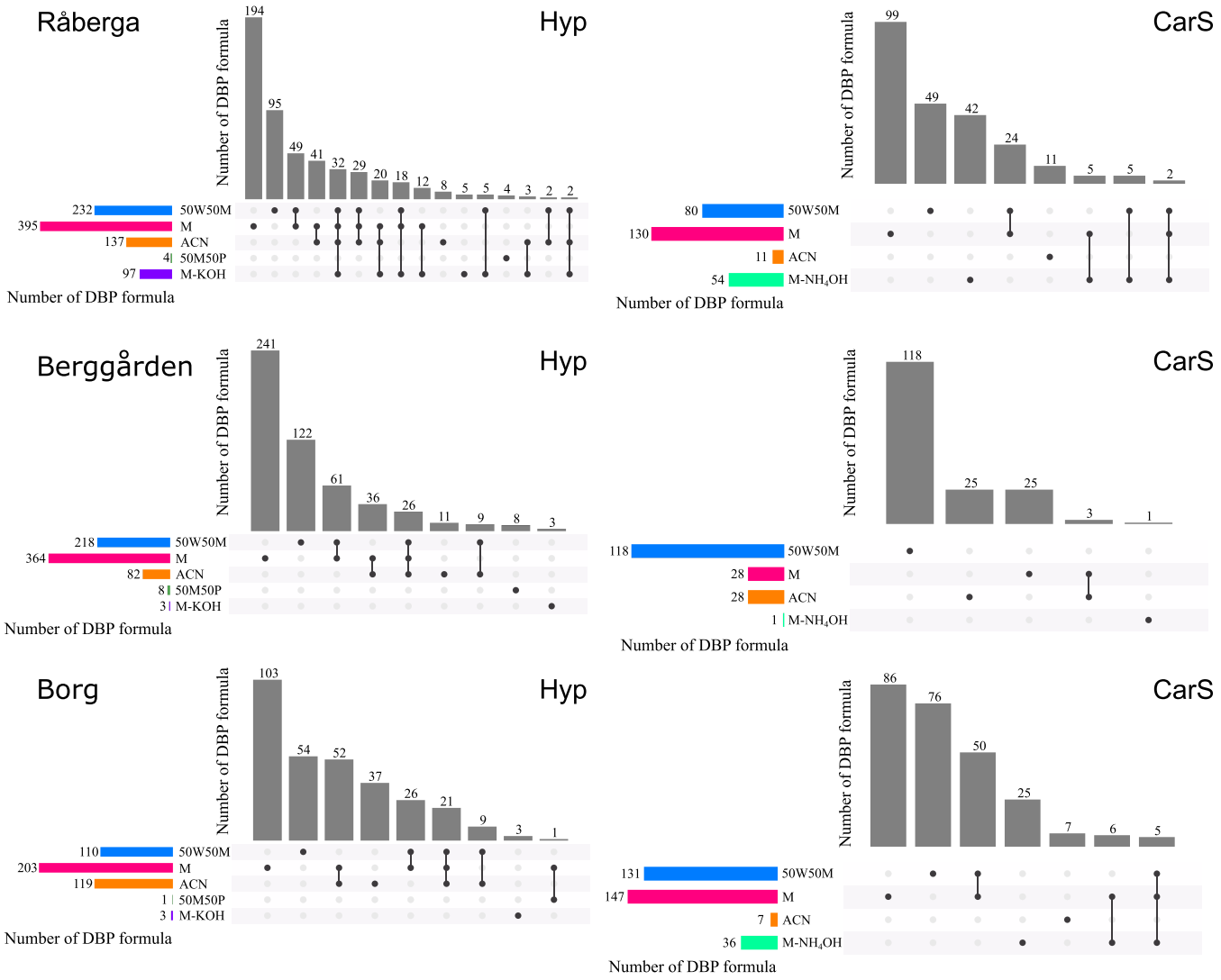

Figure 7. Overlap between DBP formulas detected in the different fractions displayed as upset plots. The colored horizontal bars represent the total numbers of DBP formulas detected in different fractions. The vertical gray bars represent the number of DBP formulas detected that were unique to a specific fraction or shared in specific combinations of fractions. Unique DBP formulas are marked with a dot, and DBP formulas detected in multiple fractions are marked with lines connecting the fractions that shared the same DBP formulas.

The verified DBP formulas detected in the different fractions at the three DWTPs are presented in Tables S2−S4.

3.3. Sample pH

Samples of final water at Borg were sequentially extracted and eluted at their original pH (pH 8.0) as well as at the low pH (pH 2.5) tested for all DWTPs. For both Hyper Sep and Carbon S fewer individual DBP formulas (114 and 31, respectively) were detected and verified at original pH compared to pH 2.5 (356 and 275, respectively) (Figures S10 and S11). However, among the DBPs detected at original pH, 44 and 65% for Hyper Sep and Carbon S, respectively, were found at natural pH only and not observed at pH 2.5.

For Hyper Sep, most DBPs detected at original pH were detected in the 50W50M and M fractions (Figure S10) while for Carbon S, the majority were found in the ACN fraction (Figure S11). For Hyper Sep, the DBPs detected at original pH were characterized by higher saturation, i.e., lower DBE, DBE/C and AI_{mod} and higher H/C, lower degree of oxygenation, i.e., lower O/C and C_{OS} compared to DBPs detected at pH 2.5. (Table S5, Table 2). Moreover, only a few Br-DBPs were observed at the original pH, indicating that they were deprotonated and thus sorbed less under slightly alkaline conditions. DBPs sorbed to Carbon S and eluted in the ACN fraction were even more saturated than those sorbed to Hyper Sep (Table S5).

pH influences DOM sorption through cation exchange on Hyper Sep, through increased occupation of cation exchange sites by H^+ as well as by influencing the protonation of DBPs.[32] At Borg very few DBPs were detected in M-KOH extracts at pH 2.5 and not a single DBP were verified at pH 8. If future extractions focus on positively charged molecules, it might be possible to optimize the retention and analysis of positively charged DBPs further through pH optimizations and ESI[+] ionization.

Overall, pH 8 resulted in the detection of saturated DBPs not detected at pH 2.5. This is consistent with a previous study focused on DBP characterization of swimming pool water at circumneutral pH and pH 2.[37] This demonstrates that extractions at the original pH can be important to cover the full image of formed DBPs. However, relative to the full assessment, DBPs detected solely at the original pH counted for 14 and 7% for Hyper Sep and Carbon S, respectively,

https://doi.org/10.1021/acsestwater.5c01469
ACS EST Water 2026, 6, 2444−2457

demonstrating a limited contribution to overall chemical diversity compared to the application of sequential extraction and elution at pH 2.5.

3.4. Comparison between Hyper Sep, Carbon S, and PPL

The DBPs captured using Hyper Sep and Carbon S were compared to those extracted by Bond Elut PPL, commonly used in DBP studies.[17] A substantially greater overlap in DBP formulas was observed between Hyper Sep and PPL extracts (42, 36, and 32%) compared to Carbon S and PPL extracts (9, 2, and 11%) for Råberga, Berggården, and Borg, respectively. Although some variation was observed across DWTPs, DBPs sorbed to PPL generally exhibited higher average oxygen content, O/C and C_{OS}, compared to those captured by Hyper Sep (Table 2 and Table S6 and Figures S7, S12, S13, and Figure 5). This suggests that the functionalized phase of PPL interacts more effectively with polar moieties in DBPs, resulting in different selectivities even among sorbents of similar reversed-phase character. However, when comparing all DBPs, 10, 19 and 17% were unique to PPL, i.e., not detected using Hyper Sep nor Carbon S, while 53, 51, and 58% were unique to sequential Hyper Sep and Carbon S extraction, i.e., not detected by sole PPL extraction for Råberga, Berggården, and Borg, respectively. Hence, integrating multiple sorbent types significantly expands the chemical space of detectable DBPs beyond what can be achieved with any one sorbent alone.

3.5. Ways Forward

Based on outcomes from this study, future efforts toward more comprehensive and convenient DBP analysis should consider the following:

(1) To improve the stepwise elution and increase the abundance of unique DBPs sorbed by a reversed-phase sorbent, the 50W50M and M fraction could be complemented with methanol mixtures with a third solvent, less polar than acetonitrile and less volatile than pentane, such as heptane or toluene. Dilution with methanol prior to analysis minimizes individual solvent impacts on DBP detection.

(2) Elution using methanol with 1 mM KOH did not enhance the diversity of DBPs detected in ESI[−] and can be excluded in future protocols with ESI[−] detection. However, the cation exchange function might be relevant when ESI is operated in positive mode, targeting nitrogen-containing DBPs.

(3) For the carbon-based sorbent, aimed to capture polar DBPs, fewer elution solvents seem needed, such as 50W50M and M. In two DWTPs 1% NH_4OH elution of the anion exchange enabled detection of distinct DBPs not covered by other fractions nor by the reversed-phase.

(4) pH is an alternative approach to separate DBPs. However, compared to the application of multiple sorbents or eluants, the impact from pH seems limited.

(5) Carbon S showed potential to sorb iodine-containing DBPs, which can be further explored by adopting alternative ways for their verification, such as iodide fragment ion analysis[45] or homologous based network analysis of iodine-containing moieties.[20] Such approaches would extend nontarget analysis of sole iodine-containing DBPs formed from high-molecular weight precursors contributing highly to toxicity,[46] comprising an important part of DBP exposure in chloraminated drinking waters containing iodide.[47]

Emerging sorbent materials which might improve selectivity for DBPs in extractions includes e.g., metal−organic frameworks[48] and graphene oxide composites[49] and complementary ionization techniques not yet investigated include ESI(+), APCI, or APPI.[17] Here we presented the fractions separately. Future work could explore pooling fractions prior to analysis, potentially improving the feasibility and applicability of sequential extraction and elution.

Compared to DBPs with one or two carbons, these DBPs have a larger surface for binding, more numerous functional groups that can cause damage, and might inherit a greater resemblance to functional large size biopolymers, i.e., being more biosimilar, which might explain their increased toxicity. Their identifications can be strengthened by combining FT-ICR MS with MS/MS and MS^3,[50] applying targeted halogen fragment ion analyses with triple quadrupole mass spectrometry[51] or by integrating ion mobility spectrometry into nontarget applications,[52] the latter has not yet been applied for DBPs. Such approaches have the potential to advance structural determination to explain the toxicological significance of the <1 kDa[53] high-molecular-weight DBPs.

4. CONCLUSIONS

Triple impacts from (1) complementary capacities of reversed-phase and carbon-based sorbents, (2) stepwise elution using solvents of different polarity, and (3) the overall influence of matrix reduction on ionization efficiency greatly extends the detected chemical diversity of nonvolatile DBPs. The approach has the potential to increase analytical windows for many emerging contaminants of concern, such as PFAS, and can be an important element in identifying key components or fractions among the overall exposure of DBPs or other contaminants in drinking water.

■ ASSOCIATED CONTENT

Supporting Information

The Supporting Information is available free of charge at https://pubs.acs.org/doi/10.1021/acsestwater.5c01469.

Additional plots presenting FT-ICR MS data, summary lists of verified DBP formulas and additional tables of average weighted compositions and indices for verified DBPs (DOCX)

■ AUTHOR INFORMATION

Corresponding Author

Anna Andersson − *Department of Thematic Studies−Environmental Change, Linköping University, SE-581 83 Linköping, Sweden;* orcid.org/0000-0002-7422-0853; Email: anna.e.andersson@liu.se

Authors

Mourad Harir − *Research Unit Analytical BioGeoChemistry, Helmholtz Munich, 85764 Neuherberg, Germany; Chair of Analytical Food Chemistry, Technical University of Munich, 85354 Freising, Germany*

Michael Gonsior − *Catalan Institute for Water Research (ICRA), 17003 Girona, Spain;* orcid.org/0000-0003-0542-4614

Norbert Hertkorn − *Department of Thematic Studies−Environmental Change, Linköping University, SE-581 83 Linköping, Sweden*

https://doi.org/10.1021/acsestwater.5c01469
ACS EST Water 2026, 6, 2444−2457

Philippe Schmitt-Kopplin − *Research Unit Analytical BioGeoChemistry, Helmholtz Munich, 85764 Neuherberg, Germany; Chair of Analytical Food Chemistry, Technical University of Munich, 85354 Freising, Germany*
Henrik Kylin − *Department of Thematic Studies−Environmental Change, Linköping University, SE-581 83 Linköping, Sweden; Research Unit: Environmental Sciences and Management, North-West University, 2520 Potchefstroom, South Africa;* orcid.org/0000-0002-5972-1852
Ämma Pettersson − *Nodra, SE-603 36 Norrköping, Sweden*
Felicia Larsson − *Tekniska Verken i Linköping AB (publ), SE-581 15 Linköping, Sweden*
David Bastviken − *Department of Thematic Studies−Environmental Change, Linköping University, SE-581 83 Linköping, Sweden;* orcid.org/0000-0003-0038-2152

Complete contact information is available at: https://pubs.acs.org/10.1021/acsestwater.5c01469

Notes

The authors declare no competing financial interest.

■ ACKNOWLEDGMENTS

We thank FORMAS, the Swedish Research Council for Sustainable Development, who funded this study (grant no. 2021-01662). We warmly thank the staff at the DWTPs, Berggården, Råberga, and Borg, for technical support during sample collection. We also thank our research engineers Susanne Karlsson and Kalpana Munnuru Singamshetty for practical assistance and good advice and Nguyen Thanh Duc for support towards implementing the upset plot.

■ REFERENCES

(1) Rook, J. J. Formation of haloforms during chlorination of natural waters. *Water Treat. Exam.* **1974**, *23*, 234−243.
(2) Villanueva, C. M.; et al. Overview of Disinfection By-products and Associated Health Effects. *Curr. Environ. Health Rep.* **2015**, *2* (1), 107−115.
(3) Save-Soderbergh, M.; Toljander, J.; Donat-Vargas, C.; Berglund, M.; Akesson, A. Exposure to drinking water chlorination by-products and fetal growth and prematurity: A nation wide register-based prospective study. *Environ. Health Perspect.* **2020**, *128* (5), No. 057006.
(4) Save-Soderbergh, M.; Toljander, J.; Donat-Vargas, C.; Akesson, A. Drinking water disinfection by-products and congenital malformations: A nationwide register-based prospective study. *Environ. Health Perspect.* **2021**, *129* (9), 97012.
(5) Li, X. F.; Mitch, W. A. Drinking Water Disinfection Byproducts (DBPs) and Human Health Effects: Multidisciplinary Challenges and Opportunities. *Environ. Sci. Technol.* **2018**, *52* (4), 1681−1689.
(6) Li, Y.; et al. Volatile DBPs contributed marginally to the developmental toxicity of drinking water DBP mixtures against Platynereis dumerilii. *Chemosphere* **2020**, *252*, 126611.
(7) Wu, Q.-Y.; Liang, Z.-F.; Wang, W.-L.; Du, Y.; Hu, H.-Y.; Yang, L.-L.; Huang, W.-C. Non-volatile disinfection byproducts are far more toxic to mammalian cells than volatile byproducts. *Water Res.* **2020**, *183*, 116080.
(8) Stalter, D.; et al. Sample Enrichment for Bioanalytical Assessment of Disinfected Drinking Water: Concentrating the Polar, the Volatiles, and the Unknowns. *Environ. Sci. Technol.* **2016**, *50* (12), 6495−6505.
(9) Lau, S. S.; et al. Regulated 1−2 Carbon Disinfection Byproducts do not Correlate with Cytotoxicity with Increasing Disinfectant Contact Time During Chlorination, Chlorination Followed by Chloramination or Granular Activated Carbon Followed by Chlorination. *Environ. Sci. Technol.* **2024**, *58* (45), 20289−20299.
(10) Chen, M.; et al. Effects of dissolved organic matter (DOM) sources and nature of solid extraction sorbent on recoverable DOM composition: Implication into potential lability of different compound groups. *Anal. Bioanal. Chem.* **2016**, *408* (17), 4809−4819.
(11) Köke, N.; et al. Multi-layer solid-phase extraction and evaporation—enrichment methods for polar organic chemicals from aqueous matrices. *Anal. Bioanal. Chem.* **2018**, *410* (9), 2403−2411.
(12) Moody, C. S. A comparison of methods for the extraction of dissolved organic matter from freshwaters. *Water Res.* **2020**, *184*, 116114.
(13) Yang, S. L.; et al. Optimization of Targeted Water Sample Extraction Methods for Different Toxicity End Points of In Vitro Bioassays. *ACS ES&T Water.* **2025**, *5* (7), 3663−3673.
(14) Lau, S. S.; et al. Disinfection Byproduct Recovery during Extraction and Concentration in Preparation for Chemical Analyses or Toxicity Assays. *Environ. Sci. Technol.* **2021**, *55* (20), 14136−14145.
(15) Badawy, M. E. I.; et al. A review of the modern principles and applications of solid-phase extraction techniques in chromatographic analysis. *Anal. Sci.* **2022**, *38* (12), 1457−1487.
(16) Phungsai, P.; et al. Changes in dissolved organic matter during water treatment by sequential solid-phase extraction and unknown screening analysis. *Chemosphere* **2021**, *263*, 128278.
(17) Andersson, A.; Harir, M.; Bastviken, D. Extending the potential of Fourier transform ion cyclotron resonance mass spectrometry for the analysis of disinfection by-products. *TrAC, Trends Anal. Chem.* **2023**, *167*, 117264.
(18) Milstead, R. P.; Remucal, C. K. Molecular-Level Insights into the Formation of Traditional and Novel Halogenated Disinfection Byproducts. *ACS ES and T Water* **2021**, *1* (8), 1966−1974.
(19) Gonsior, M.; et al. Changes in Dissolved Organic Matter during the Treatment Processes of a Drinking Water Plant in Sweden and Formation of Previously Unknown Disinfection Byproducts. *Environ. Sci. Technol.* **2014**, *48* (21), 12714−12722.
(20) Fu, Q. L.; et al. Formula Assignment Algorithm for Deuterium-Labeled Ultrahigh-Resolution Mass Spectrometry: Implications of the Formation Mechanism of Halogenated Disinfection Byproducts. *Anal. Chem.* **2022**, *94* (3), 1717−1725.
(21) Li, Y.; et al. Comprehensive structure-selective characterization of dissolved organic matter by reducing molecular complexity and increasing analytical dimensions. *Water Res.* **2016**, *106*, 477−487.
(22) Lv, J.; et al. Solid-phase extraction-stepwise elution (SPE-SE) procedure for isolation of dissolved organic matter prior to ESI-FT-ICR-MS analysis. *Anal. Chim. Acta* **2016**, *948*, 55−61.
(23) Gao, Y.; et al. Fractionation and molecular characterization of natural organic matter (NOM) by solid-phase extraction followed by FT-ICR MS and ion mobility MS. *Anal. Bioanal. Chem.* **2019**, *411* (24), 6343−6352.
(24) Wang, C.; et al. Deciphering molecular composition and summarizing control strategies of unknown disinfection by-products in water and wastewater based on FT-ICR-MS analysis: a comprehensive review. *Environ. Sci.: Water Res. Technol.* **2025**, *11* (3), 573−589.
(25) Wu, S.; Fujii, M.; Yang, X.; Fu, Q.-L. Characterization of halogenated organic compounds by the Fourier transform ion cyclotron resonance mass spectrometry: A critical review. *Water Res.* **2023**, *246*, 120694.
(26) Andersson, A.; et al. Waterworks-specific composition of drinking water disinfection by-products. *Environ. Sci.: Water Res. Technol.* **2019**, *5* (5), 861−872.
(27) Andersson, A.; et al. Selective removal of natural organic matter during drinking water production changes the composition of disinfection by-products. *Environ. Sci.: Water Res. Technol.* **2020**, *6* (3), 779−794.
(28) Gonsior, M.; et al. The chemodiversity of algal dissolved organic matter from lysed Microcystis aeruginosa cells and its ability to form disinfection by-products during chlorination. *Water Res.* **2019**, *155*, 300−309.
(29) Lavonen, E. E.; et al. Selective chlorination of natural organic matter: Identification of previously unknown disinfection byproducts. *Environ. Sci. Technol.* **2013**, *47* (5), 2264−2271.

(30) Zhang, H.; et al. Study on transformation of natural organic matter in source water during chlorination and its chlorinated products using ultrahigh resolution mass spectrometry. *Environ. Sci. Technol.* **2012**, *46* (8), 4396−4402.
(31) Zhang, H.; et al. Characterization of low molecular weight dissolved natural organic matter along the treatment trait of a waterworks using Fourier transform ion cyclotron resonance mass spectrometry. *Water Res.* **2012**, *46* (16), 5197−5204.
(32) Stücheli, P. E.; Niggemann, J.; Schubert, C. J. Comparison of different solid phase extraction sorbents for the qualitative assessment of dissolved organic nitrogen in freshwater samples using FT-ICR-MS. *J. Limnol.* **2015**, *77* (3), 400−411.
(33) Plewa, M. J.; Wagner, E. D.; Muellner, M. G.; Hsu, K.-M.; Richardson, S. D. Comparative mammalian cell toxicity of N-DBPs and C-DBPs. In *Disinfection By-Products in Drinking Water*; ACS Symposium Series; American Chemical Society: Washington DC, 2008; Vol. *995*, pp 36−50.
(34) Plewa, M. J.; Wagner, E. D.; Richardson, S. D. TIC-Tox: A preliminary discussion on identifying the forcing agents of DBP-mediated toxicity of disinfected water. *J. Environ. Sci. (China)* **2017**, *58*, 208−216.
(35) Godinho, J. M.; Naese, J. A.; Toler, A. E.; Boyes, B. E.; Henry, R. A.; DeStefano, J. J.; Grinias, J. P. Importance of Particle Pore Size in Determining Retention and Selectivity in Reversed Phase Liquid Chromatography. *J. Chromatogr. A* **2020**, *1634*, 461678.
(36) Hertkorn, N.; et al. Natural organic matter and the event horizon of mass spectrometry. *Anal. Chem.* **2008**, *80* (23), 8908−8919.
(37) Qin, R.; et al. Improved identification of chlorinated disinfection byproducts by the sequential elution and absorption mode. *J. Hazard. Mater.* **2025**, *493*, 138337.
(38) Andersson, A.; et al. Molecular changes among non-volatile disinfection by-products between drinking water treatment and consumer taps. *Environ. Sci.: Water Res. Technol.* **2021**, *7* (12), 2335−2345.
(39) Herzsprung, P.; et al. Understanding molecular formula assignment of Fourier transform ion cyclotron resonance mass spectrometry data of natural organic matter from a chemical point of view. *Anal. Bioanal. Chem.* **2014**, *406* (30), 7977−7987.
(40) Koch, B. P.; Dittmar, T. From mass to structure: An aromaticity index for high-resolution mass data of natural organic matter. *Rapid Commun. Mass Spectrom.* **2006**, *20* (5), 926−932.
(41) Kroll, J. H.; et al. Carbon oxidation state as a metric for describing the chemistry of atmospheric organic aerosol. *Nat. Chem.* **2011**, *3* (2), 133−139.
(42) Andersson, A.; et al. Molecular level seasonality of dissolved organic matter in freshwater and its impact on drinking water treatment. *Environ. Sci.: Water Res. Technol.* **2024**, *10* (8), 1964−1981.
(43) Wagner, E. D.; Plewa, M. J. CHO cell cytotoxicity and genotoxicity analyses of disinfection by-products: An updated review. *J. Environ. Sci. (China)* **2017**, *58*, 64−76.
(44) Leyva, D.; et al. Understanding the structural complexity of dissolved organic matter: Isomeric diversity. *Faraday Discuss.* **2019**, *218*, 431−440.
(45) Luek, J. L.; et al. Halogenated Organic Compounds Identified in Hydraulic Fracturing Wastewaters Using Ultrahigh Resolution Mass Spectrometry. *Environ. Sci. Technol.* **2017**, *51* (10), 5377−5385.
(46) Yang, W.; et al. High Molecular-Weight Organics as Precursors for Toxic Iodinated Disinfection Byproducts during Chloramination. *Environ. Sci. Technol.* **2025**, *59* (2), 1378−1387.
(47) Niehaves, E.; Justen, P. T.; Perkins, A. A.; Forster, A. L.B.; Granger, C. O.; Richardson, S. D. Chasing disinfection byproducts through the pipes: How 66 DBPs change over time in chlorinated vs. chloraminated distribution systems. *Water Res.* **2026**, *289*, 124813.
(48) Firooz, S. K.; Armstrong, D.W. Metal-organic frameworks in separations: A review. *Anal. Chim. Acta* **2022**, *1234*, 340208.
(49) Li, H.; et al. Molecular separation applications of next-generation graphene oxide composite membranes with enhanced properties: Current status and future prospects. *Sep. Purif. Technol.* **2025**, *358*, 130451.
(50) Liberatore, H. K.; et al. High-Resolution Mass Spectrometry Identification of Novel Surfactant-Derived Sulfur-Containing Disinfection Byproducts from Gas Extraction Wastewater. *Environ. Sci. Technol.* **2020**, *54* (15), 9374−9386.
(51) Yang, M.; et al. Application of (LC/)MS/MS precursor ion scan for evaluating the occurrence, formation and control of polar halogenated DBPs in disinfected waters: A review. *Water Res.* **2019**, *158*, 322−337.
(52) Postigo, C.; Richardson, S.D. Non-target screening and novel methods based on mass spectrometry detection for identification of unknown disinfection byproducts. *Compr. Anal. Chem.* **2021**, *97*, 1−29.
(53) Dong, H.; Cuthbertson, A. A.; Plewa, M. J.; Weisbrod, C. R.; McKenna, A. M.; Richardson, S. D. Unravelling High-Molecular-Weight DBP Toxicity Drivers in Chlorinated and Chloraminated Drinking Water: Effect-Directed Analysis of Molecular Weight Fractions. *Environ. Sci. Technol.* **2023**, *57*, 18788.